

A Common Origin for Cosmic Explosions Inferred from Fireball Calorimetry

E. Berger¹, S. R. Kulkarni¹, G. Pooley², D. A. Frail³, V. McIntyre⁴,
R. M. Wark⁵, R. Sari⁶, A. M. Soderberg¹, D. W. Fox¹, S. Yost⁷, P. A. Price⁸

¹ Caltech Optical Observatories 105-24, California Institute of Technology, Pasadena, CA 91125, USA

² Mullard Radio Astronomy Observatory, Cavendish Lab., Madingley Road, Cambridge CB3 0HE, UK

³ National Radio Astronomy Observatory, P.O. Box 0, Socorro, New Mexico 87801, USA

⁴ Australia Telescope National Facility, CSIRO, P.O. Box 76, Epping, NSW 1710, Australia

⁵ Australia Telescope National Facility, CSIRO, Locked Bag 194, Narrabri NSW 2390, Australia

⁶ Theoretical Astrophysics 130-33, California Institute of Technology, Pasadena, CA 91125, USA

⁷ Space Radiation Laboratory 220-47, California Institute of Technology, Pasadena, CA 91125, USA

⁸ RSAA, ANU, Mt. Stromlo Observatory, via Cotter Rd, Weston Creek, ACT, 2611, Australia

Past studies¹⁻³ suggest that long-duration γ -ray bursts (GRBs) have a standard energy of $E_\gamma \sim 10^{51}$ erg in ultra-relativistic ejecta when corrected for asymmetry (“jets”). However, recently^{2,3} a group of sub-energetic bursts, including the peculiar GRB 980425 associated⁴ with SN 1998bw ($E_\gamma \approx 10^{48}$ erg), has been identified. Here we report radio observations of GRB 030329, the nearest burst to date, which allow us to undertake calorimetry of the explosion. Our observations require a two-component explosion: a narrow (5°) ultra-relativistic component responsible for the γ -rays and early afterglow, and a wide, mildly relativistic component responsible for the radio and optical afterglow beyond 1.5 days. While the γ -rays are energetically minor, the total energy release, dominated by the wide component, is similar^{1-3,5} to that of other GRBs. Given the firm link^{6,7} of GRB 030329 with SN 2003dh our result suggests a common origin for cosmic explosions in which, for reasons not understood, the energy in the highest velocity ejecta is highly variable.

We initiated observations of the nearby GRB 030329 ($z = 0.1685$) in the centimetre band approximately 13.8 hours after the burst. The log of the observations and the resulting lightcurves are displayed in Tables 1 and 2 and Figure 1. The afterglow was also observed extensively in the millimetre (100 GHz) and sub-millimetre (250 GHz) bands.⁸ While this is the brightest radio afterglow detected to date, the low redshift results in a

peak luminosity, $L_{\nu,p}(8.5 \text{ GHz}) \approx 1.8 \times 10^{31} \text{ erg s}^{-1} \text{ Hz}^{-1}$, typical⁹ of other long-duration GRBs.

The observed rapid decline, $F_\nu \propto t^{-1.9}$ at $t \gtrsim 10 \text{ d}$ and the decrease in peak flux at $\nu \lesssim 22.5 \text{ GHz}$ (Figure 1) are the hallmarks of a collimated explosion. In this framework,¹⁰ the sharp decline (or “jet break”) occurs at the time, t_j , when $\Gamma(t_j) \sim \theta_j^{-1}$ due to relativistic aberration (“beaming”) and rapid side-ways expansion; here Γ is the bulk Lorentz factor and θ_j is the opening angle of the jet. We model the afterglow emission (cf. ref. 5,11) from 4.9 to 250 GHz assuming a uniform¹⁰ as well as a “wind”¹² (particle density profile, $\rho \propto r^{-2}$, where r is the distance from the source) circumburst medium. Neither model is strongly preferred, but $t_{j,\text{rad}} \approx 9.8 \text{ d}$ is required (Figure 1).

Using the inferred particle density of $n \approx 1.8 \text{ cm}^{-3}$ and assuming a γ -ray efficiency, $\epsilon_\gamma = 0.2$ (see ref. 3) we infer $\theta_{j,\text{rad}} \sim 0.3 \text{ rad}$, or 17° . The kinetic energy in the explosion corrected for collimation is $E_K = f_b E_{K,\text{iso}} \approx 2.5 \times 10^{50} \text{ erg}$, where $f_b = [1 - \cos(\theta_j)]$ is the beaming fraction and $E_{K,\text{iso}}$ is the isotropic equivalent kinetic energy. This value is comparable to that inferred from modeling of other afterglows.⁵

In contrast to the above discussion, Price et al.¹³ note a sharp break in the optical afterglow at $t = 0.55 \text{ d}$ (Figure 2). The X-ray flux¹⁴ tracks the optical afterglow for the first day, with a break consistent with that seen in the optical. Thus the break at 0.55 d is not due to a change in the ambient density since for typical parameters^{15,16} the X-ray emission is not sensitive to density. However, unlike the optical emission the X-ray flux at later times continues to decrease monotonically. Thus we conclude that there are two emitting components: one responsible for the early optical and X-ray emission and the other responsible for the optical emission beyond 1.5 days.

The first component, given the characteristic t^{-2} decay for both the X-ray and optical emission, is reasonably modeled by a jet. For the parameters used above (n , ϵ_γ) the opening angle is 0.09 rad or 5° .

The resurgence in the optical emission at 1.5 d requires a second component. An increase in the ambient density cannot explain this resurgence since the predicted decrease in radio luminosity, arising from the increase in synchrotron self-absorption, is not observed (Figure 1). An increase in the energy of the first component, for example by

successive shells with lower Lorentz factors as advocated by Granot et al.,¹⁷ is ruled out by the lack⁸ of strong radio or millimetric emission expected¹⁸ from reverse shocks.

Thus, by a process of elimination, we are led to a two-component explosion model in which the first component (a narrow jet, 5°) with initially larger Γ is responsible for the γ -ray burst and the early optical and X-ray afterglow including the break at 0.55 d, while the second component (a wider jet, 17°) powers the radio afterglow and late optical emission (Figure 2). The break due to the second component is readily seen in the radio afterglow, but is masked by SN 2003dh in the optical bands, thus requiring careful subtraction (Figure 2). Such a two-component jet finds a natural explanation in the collapsar model.¹⁹

The beaming-corrected γ -ray energy, emitted by the narrow jet, is only $E_\gamma \approx 5 \times 10^{49}$ erg, significantly lower than the strong clustering³ around 1.3×10^{51} erg seen in most bursts. Similarly, the beaming-corrected X-ray luminosity¹⁴ at $t = 10$ hours, a proxy for the kinetic energy of the afterglow on that timescale, is $L_{X,10} \approx 3 \times 10^{43}$ erg s⁻¹, a factor of ten below the tightly clustered values² for most other bursts. However, the second component, which is mildly relativistic (as determined by the lower energy peak of its spectrum), carries the bulk of the energy, as indicated by our modeling of the radio emission. We note that our model, with the energy in the lower Lorentz factor component dominating over the narrow ultra-relativistic component, is not consistent with “universal standard jet” model.²⁰

The afterglow calorimetry presented here has important ramifications for our understanding of GRB engines. Recently, we have come to recognize a sub-class of cosmological GRBs marked by rapidly fading afterglows at early time (i.e. similar to GRB 030329). These events are sub-energetic^{2,3} in E_γ and early X-ray afterglow luminosity. However, as demonstrated by our calorimetry of GRB 030329, such bursts may have total explosive yields similar to other GRBs (Figure 3).

This leads to the following conclusions. First, radio calorimetry, which is sensitive to all ejecta with $\Gamma \gtrsim few$, shows that the explosive yield of the nearest “classical” event, GRB 030329, is dominated by mildly relativistic ejecta. Ultra-relativistic ejecta which produced the γ -ray emission is energetically unimportant. Second, the total energy yield of GRB 030329 is similar to those estimated for other bursts. Along these lines, the enigmatic

GRB 980425 associated⁴ with the nearby supernova SN 1998bw also has negligible γ -ray emission, $E_{\gamma,\text{iso}} \approx 8 \times 10^{47}$ erg; however, radio calorimetry²¹ shows that even this extreme event had a similar explosive energy yield (Figure 3). The newly recognized class of cosmic explosions, the X-ray Flashes,²² exhibit little or no γ -ray emission but appear to have comparable X-ray and radio afterglows to those of GRBs. Thus, the commonality of the total energy yield indicates a common origin, but apparently the ultra-relativistic output is highly variable. Unraveling what physical parameter is responsible for the variation in the “purity” (ultra-relativistic output) of the engine appears to be the next frontier in the field of cosmic explosions.

Received 3 September 2018; Accepted **draft**.

1. Frail, D. A., Kulkarni, S. R., Sari, R., Djorgovski, S. G., Bloom, J. S. *et al.* Beaming in Gamma-Ray Bursts: Evidence for a Standard Energy Reservoir. *Astrophys. J.* **562**, L55–L58 November 2001.
2. Berger, E., Kulkarni, S. R. & Frail, D. A. A Standard Kinetic Energy Reservoir in Gamma-Ray Burst Afterglows. *Astrophys. J.* **590**, 379–385 June 2003.
3. Bloom, J. S., Frail, D. A. & Kulkarni, S. R. GRB Energetics and the GRB Hubble Diagram: Promises and Limitations. *ArXiv Astrophysics e-prints*, 2210–+ February 2003.
4. Galama, T. J., Vreeswijk, P. M., van Paradijs, J., Kouveliotou, C., Augusteijn, T. *et al.* An unusual supernova in the error box of the gamma-ray burst of 25 April 1998. *Nature* **395**, 670–672 (1998).
5. Panaitescu, A. & Kumar, P. Properties of Relativistic Jets in Gamma-Ray Burst Afterglows. *Astrophys. J.* **571**, 779–789 June 2002.
6. Stanek, K. Z., Matheson, T., Garnavich, P. M., Martini, P., Berlind, P. *et al.* Spectroscopic Discovery of the Supernova 2003dh Associated with GRB 030329. *ArXiv Astrophysics e-prints*, 4173–+ April 2003.
7. Hjorth, J. & *et al.* A very energetic supernova associated with the gamma-ray burst of 29 March 2003. *Nature* in press (2003).
8. Sheth, K., Frail, D. A., White, S., Das, M., Bertoldi, F. *et al.* GRB 030329 at millimeter wavelengths: OVRO, BIMA, & MAMBO Observations. Submitted to *ApJ* (2003).

9. Frail, D. A., Kulkarni, S. R., Berger, E. & Wieringa, M. H. A Complete Catalog of Radio Afterglows: The First Five Years. *Astron. J.* **125**, 2299–2306 May 2003.
10. Sari, R., Piran, T. & Halpern, J. P. Jets in Gamma-Ray Bursts. *Astrophys. J.* **519**, L17–L20 July 1999.
11. Berger, E., Sari, R., Frail, D. A., Kulkarni, S. R., Bertoldi, F. *et al.* A Jet Model for the Afterglow Emission from GRB 000301C. *Astrophys. J.* **545**, 56–62 December 2000.
12. Chevalier, R. A. & Li, Z. Wind Interaction Models for Gamma-Ray Burst Afterglows: The Case for Two Types of Progenitors. *Astrophys. J.* **536**, 195–212 June 2000.
13. Price, P. A., Fox, D. W., Kulkarni, S. R., Peterson, B. A., Schmidt, B. P. *et al.* Discovery of the Bright Afterglow of the Nearby Gamma-Ray Burst of 29 March 2003. Nature in press (2003).
14. Tiengo, A., Mereghetti, S., Ghisellini, G., Rossi, E., Ghirlanda, G. *et al.* The X-ray afterglow of GRB030329. *ArXiv Astrophysics e-prints*, 5564+ May 2003.
15. Kumar, P. The Distribution of Burst Energy and Shock Parameters for Gamma-Ray Bursts. *apjl* **538**, L125–L128 August 2000.
16. Freedman, D. L. & Waxman, E. On the Energy of Gamma-Ray Bursts. *Astrophys. J.* **547**, 922–928 February 2001.
17. Granot, J., Nakar, E. & Piran, T. The Variable Light Curve of GRB 030329: The Case for Refreshed Shocks. *ArXiv Astrophysics e-prints*, 4563+ April 2003.
18. Sari, R. & Mészáros, P. Impulsive and Varying Injection in Gamma-Ray Burst Afterglows. *Astrophys. J.* **535**, L33–L37 May 2000.
19. MacFadyen, A. I., Woosley, S. E. & Heger, A. Supernovae, Jets, and Collapsars. *Astrophys. J.* **550**, 410–425 March 2001.
20. Rossi, E., Lazzati, D. & Rees, M. J. Afterglow light curves, viewing angle and the jet structure of γ -ray bursts. *Mon. Not. R. astr. Soc.* **332**, 945–950 June 2002.
21. Li, Z. & Chevalier, R. A. Radio Supernova SN 1998BW and Its Relation to GRB 980425. *Astrophys. J.* **526**, 716–726 December 1999.
22. Heise, J., in 't Zand, J. J. M. & Kulkarni, S. R. X-ray Flashes: A New Class of Cosmic Explosions. in prep. (2003).

23. Galama, T. J., Frail, D. A., Sari, R., Berger, E., Taylor, G. B. *et al.* Continued Radio Monitoring of the Gamma-Ray Burst 991208. *Astrophys. J.* **585**, 899–907 March 2003.
 24. Sari, R. & Esin, A. A. On the Synchrotron Self-Compton Emission from Relativistic Shocks and Its Implications for Gamma-Ray Burst Afterglows. *Astrophys. J.* **548**, 787–799 February 2001.
 25. Henden, A., Canzian, B., Zeh, A. & Klose, S. GRB 030329, light curve flattens. *GRB Circular Network* **2123**, 1–+ (2003).
 26. Ibrahimov, M. A., Asfandiyarov, I. M., Kahharov, B. B., Pozanenko, A., Rumyantsev, V. *et al.* GRB 030329, BVRI photometry. *GRB Circular Network* **2191**, 1–+ (2003).
 27. Testa, V., Cocozza, G., Melandri, A., Antonelli, L. A., Malesani, D. *et al.* GRB 030329: VR Photometry at TNG. *GRB Circular Network* **2141**, 1–+ (2003).
-

Acknowledgements

GRB research at Caltech is supported in part by funds from NSF and NASA. We are, as always, indebted to Scott Barthelmy and the GCN. The VLA is operated by the National Radio Astronomy Observatory, a facility of the National Science Foundation operated under cooperative agreement by Associated Universities, Inc. The Australia Telescope is funded by the Commonwealth of Australia for operations as a National Facility managed by CSIRO. The Ryle Telescope is supported by PPARC.

Epoch (UT)	Δt (days)	$F_{1.43}$ (mJy)	$F_{4.86}$ (mJy)	$F_{8.46}$ (mJy)	$F_{15.0}$ (mJy)	$F_{22.5}$ (mJy)	$F_{43.3}$ (mJy)
Mar 30.06	0.58	—	—	3.50 ± 0.06	—	—	—
Mar 30.53	1.05	—	0.54 ± 0.13	1.98 ± 0.17	—	—	—
Apr 1.13	2.65	< 0.21	3.45 ± 0.05	8.50 ± 0.05	19.68 ± 0.14	30.40 ± 0.06	46.63 ± 0.18
Apr 2.05	3.57	< 0.30	1.51 ± 0.05	6.11 ± 0.04	16.98 ± 0.19	31.59 ± 0.14	44.17 ± 0.35
Apr 3.21	4.76	< 0.36	3.58 ± 0.04	9.68 ± 0.03	22.59 ± 0.12	35.57 ± 0.09	46.32 ± 0.23
Apr 5.37	6.89	< 0.40	6.77 ± 0.08	15.56 ± 0.06	28.58 ± 0.20	44.09 ± 0.15	55.33 ± 0.43
Apr 6.16	7.68	< 0.25	5.34 ± 0.10	12.55 ± 0.21	27.26 ± 0.21	39.68 ± 0.20	43.81 ± 1.00
Apr 7.97	9.49	< 0.68	3.55 ± 0.11	13.58 ± 0.09	28.50 ± 0.23	48.16 ± 0.23	43.06 ± 1.33
Apr 10.38	11.90	< 0.58	7.51 ± 0.08	17.70 ± 0.05	31.40 ± 0.25	42.50 ± 0.14	37.86 ± 0.46
Apr 11.17	12.69	—	7.42 ± 0.09	17.28 ± 0.10	29.60 ± 0.29	36.84 ± 0.16	31.26 ± 0.51
Apr 13.35	14.87	—	9.49 ± 0.13	19.15 ± 0.08	26.78 ± 0.33	32.69 ± 0.13	25.44 ± 0.51
Apr 15.14	16.66	—	8.21 ± 0.08	17.77 ± 0.10	24.50 ± 0.31	—	17.10 ± 0.71
Apr 17.20	18.72	< 0.63	6.50 ± 0.11	15.92 ± 0.07	22.02 ± 0.25	22.41 ± 0.08	18.07 ± 0.28
Apr 19.06	20.58	—	8.66 ± 0.10	16.08 ± 0.06	18.35 ± 0.24	18.03 ± 0.11	13.15 ± 0.29
Apr 24.18	25.70	—	10.04 ± 0.08	15.34 ± 0.06	13.93 ± 0.26	13.63 ± 0.13	8.54 ± 0.48
Apr 26.92	28.44	< 0.58	8.05 ± 0.08	12.67 ± 0.09	11.82 ± 0.26	9.75 ± 0.23	5.95 ± 0.62
Apr 28.96	30.48	—	—	—	10.40 ± 0.33	9.53 ± 0.21	—
Apr 29.99	31.51	—	9.80 ± 0.09	13.55 ± 0.07	—	—	—
May 2.06	33.58	—	11.62 ± 0.08	13.10 ± 0.06	—	9.52 ± 0.14	—
May 3.07	34.59	—	—	—	—	—	5.30 ± 0.32
May 5.00	36.52	—	8.90 ± 0.08	10.64 ± 0.06	8.58 ± 0.17	7.20 ± 0.09	3.75 ± 0.26
May 11.03	42.55	—	7.72 ± 0.13	8.04 ± 0.08	7.03 ± 0.19	—	—
May 13.03	44.55	—	8.57 ± 0.09	8.68 ± 0.08	5.77 ± 0.22	5.75 ± 0.10	—
May 14.00	45.52	—	—	—	—	5.23 ± 0.17	2.84 ± 0.23
May 28.03	59.55	—	6.08 ± 0.10	4.48 ± 0.09	2.82 ± 0.21	2.84 ± 0.20	—
June 4.01	66.53	1.94 ± 0.06	6.20 ± 0.08	4.93 ± 0.06	—	2.56 ± 0.12	—

Table 1. Radio observations made with the Very Large Array (VLA) and the Australia Telescope Compact Array (ATCA). Observations commenced on March 30.06 UT with a single 7-hour observation with ATCA on Mar. 30.53 UT. In the initial observation we detected a point source at $\alpha(\text{J2000})=10^{\text{h}}44^{\text{m}}49.95^{\text{s}}$, $\delta(\text{J2000})=21^{\circ}31'17.38''$, with an uncertainty of about 0.1 arcsec in each coordinate, consistent with the position of the optical counterpart. In all VLA observations we used the standard continuum mode with 2×50 MHz bands. At 22.5 and 43.3 GHz we used referenced pointing scans to correct for the systematic 10 – 20 arcsec pointing errors of the VLA antennas. We used the extra-galactic sources 3C 147 (J0542+498) and 3C 286 (J1331+305) for flux calibration, while the phase was monitored using J1111+199 at 1.43 GHz and J1051+213 at all other frequencies. The ATCA observations were performed at 4.80, 6.21, 8.26, and 9.02 GHz with a bandwidth of 64 MHz in each frequency. The phase was monitored using J1049+215, while the flux was calibrated using J1934-638. The data were reduced and analyzed using the Astronomical Image Processing System (AIPS) and the Multichannel Image Reconstruction, Image Analysis and Display package (MIRIAD). The flux density and uncertainty were measured from the resulting maps by fitting a Gaussian model to the afterglow. In addition to the rms noise in each measurement we estimate a systematic uncertainty of about 2% due to uncertainty in the absolute flux calibration.

Epoch (UT)	Δt (days)	$F_{15.3}$ (mJy)	Epoch (UT)	Δt (days)	$F_{15.3}$ (mJy)
Mar 30.91	1.43	10.38 ± 0.28	Apr 21.72	23.24	17.63 ± 0.29
Mar 31.12	1.64	13.05 ± 0.28	Apr 22.66	24.18	14.51 ± 0.49
Mar 31.91	2.43	18.66 ± 0.28	Apr 23.33	24.85	14.62 ± 0.49
Apr 1.12	2.64	18.29 ± 0.28	Apr 25.81	27.33	13.60 ± 0.65
Apr 1.98	3.50	16.75 ± 0.27	Apr 26.82	28.34	11.78 ± 0.52
Apr 3.07	4.59	20.36 ± 0.45	Apr 29.82	31.34	10.35 ± 0.49
Apr 4.09	5.61	29.13 ± 0.52	May 1.63	33.15	8.73 ± 0.52
Apr 4.97	6.49	27.97 ± 0.26	May 4.80	36.32	9.15 ± 0.50
Apr 5.97	7.49	28.69 ± 0.26	May 6.83	38.35	7.87 ± 0.50
Apr 7.06	8.58	29.29 ± 0.49	May 8.73	40.25	6.70 ± 0.50
Apr 7.89	9.41	29.15 ± 0.44	May 10.76	42.28	6.49 ± 0.50
Apr 9.89	11.41	30.78 ± 0.51	May 15.76	47.28	5.74 ± 0.50
Apr 11.05	12.57	28.52 ± 0.51	May 20.70	52.22	5.69 ± 0.53
Apr 11.88	13.40	29.92 ± 0.44	May 22.76	54.28	4.78 ± 0.78
Apr 13.05	14.57	27.90 ± 0.44	May 24.76	56.28	4.31 ± 0.55
Apr 13.87	15.39	24.74 ± 0.44	May 25.56	57.08	5.04 ± 0.84
Apr 14.82	16.34	23.60 ± 0.32	May 26.75	58.27	3.99 ± 0.63
Apr 16.96	18.48	23.06 ± 0.24	May 28.76	60.28	3.96 ± 0.58
Apr 17.92	19.44	20.51 ± 0.24	May 29.82	61.34	4.35 ± 0.50
Apr 19.95	21.47	19.27 ± 0.38	May 30.76	62.28	2.65 ± 0.72
Apr 20.72	22.24	17.53 ± 0.33	June 2.54	64.06	3.13 ± 0.76

Table 2. Radio observations at 15.3 GHz made with the Ryle Telescope at Cambridge (UK). All observations were made by interleaving 15 minutes scans of GRB 030329 with 2.5 minutes scans of the phase calibrator J1051+2119. The absolute flux scale was calibrated using 3C 48 and 3C 286. We used 5 antennas providing 10 baselines in the range 35 – 140 m. Since the position of the source is well known the in-phase component of the vector sum of the 10 baselines was used as an unbiased estimate of the flux density. The typical rms fluctuation on the signal in a 32-s integration period is approximately 6 mJy. We also add a systematic uncertainty of about 2% due to uncertainty in the absolute flux calibration.

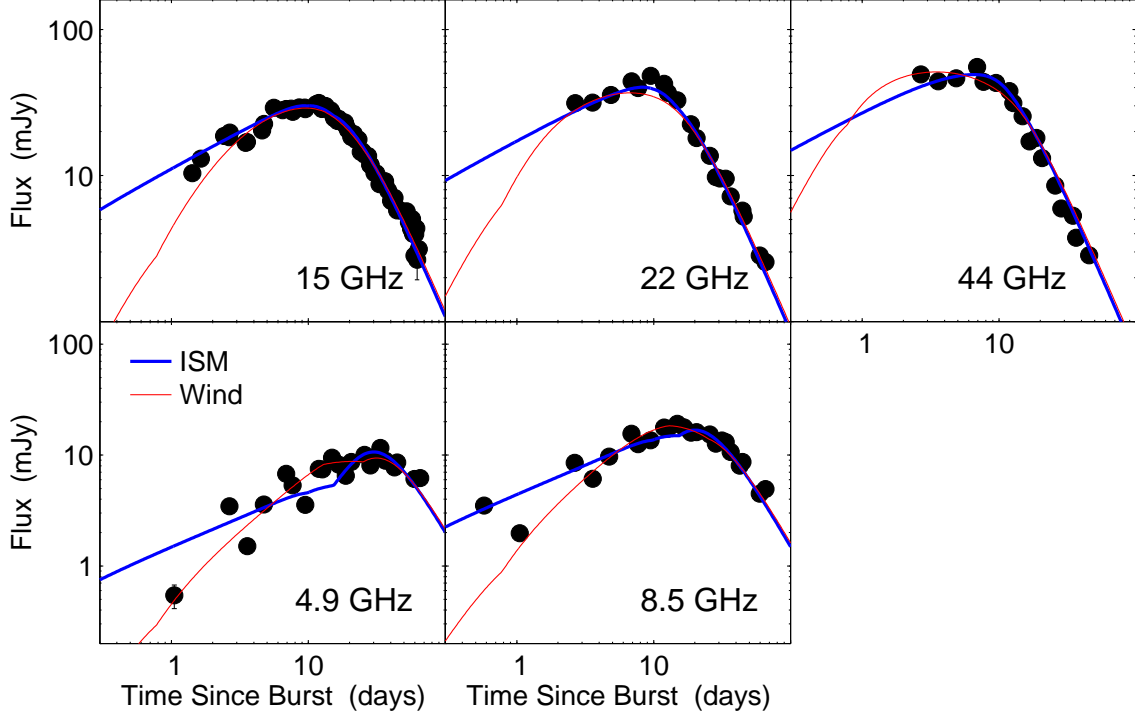


Figure 1. Radio lightcurves of the afterglow of GRB 030329. All measurements include 1σ error bars which in most cases are smaller than the symbols. The data are summarized in Tables 1 and 2. The solid lines are models of synchrotron emission from collimated relativistic ejecta expanding into uniform¹⁰ (thick) and wind¹² $\rho \propto r^{-2}$ (thin) circumburst media; these models include the millimetre and sub-millimetre data.⁸ We find $\chi_r^2 = 31.3$ and 39.8 (164 degrees of freedom) for the uniform density and wind models, respectively; these include a 2% systematic error added in quadrature to each measurement. The large values of χ_r^2 are dominated by interstellar scintillation (ISS) at $\nu \lesssim 15$ GHz and mild deviations from the expected smooth behavior at the high frequencies. Comparing the data and models, we find rms flux modulations of 0.25 at 4.9 GHz, 0.15 at 8.5 GHz, and 0.08 at 15 GHz, as well as a drop by a factor of three in the level of modulation from ~ 3 to 40 days. These properties are expected in weak ISS as the fireball expands on the sky. The inferred source size of about $20 \mu\text{as}$ (i.e. $\sim 2 \times 10^{17}$ cm) at $t \sim 15$ days is in close agreement with theoretical expectations.²³ In the uniform density model the jet break occurs at $t \approx 10$ d corresponding to an opening angle, $\theta_j \approx 0.3$ (17°). From the derived synchrotron parameters (at $t = t_j$): $\nu_a \approx 19$ GHz, $\nu_m \approx 43$ GHz, $F_{\nu,m} \approx 96$ mJy we find an isotropic kinetic energy, $E_{K,\text{iso}} \approx 5.6 \times 10^{51} \nu_{c,13}^{1/4}$ erg, a circumburst density $n = 1.8 \nu_{c,13}^{3/4} \text{ cm}^{-3}$, and the fractions of energy in the relativistic electrons and magnetic field of $0.16 \nu_{c,13}^{1/4}$ and $0.10 \nu_{c,13}^{-5/4}$, respectively; here $\nu_c = 10^{13} \nu_{c,13}$ is the synchrotron cooling frequency, and a constraint on Inverse Compton cooling as advocated by Sari & Esin²⁴ indicates $\nu_{c,13} \lesssim 1$. The beaming-corrected kinetic energy is $E_K \approx 2.5 \times 10^{50} \nu_{c,13}^{1/4}$ erg, typical of other well-studied long-duration GRBs.⁵ The parameters derived from the wind model are consistent with those from the uniform density model to within 10%.

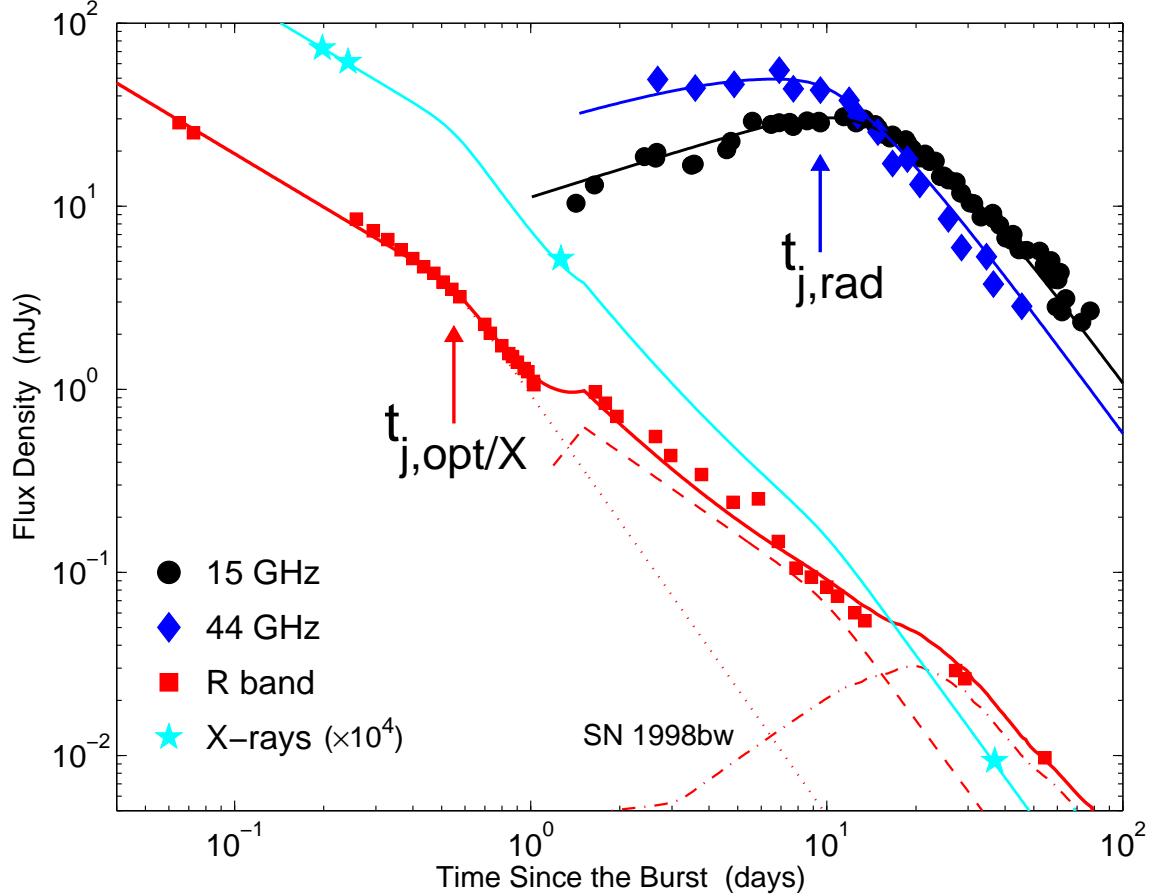


Figure 2. Radio to X-ray lightcurves of the afterglow of GRB 030329. The optical data, from Price et al.¹³ and the GRB Coordinates Network,^{25–27} have been corrected for Galactic extinction, $A_R = 0.067$ mag; we note that the latter are preliminary data. The dotted line is the model proposed by Price et al.¹³ for the early optical emission, with $t_{j,\text{opt}} \approx 0.55$ d. The dashed line is an extrapolation of the uniform density model presented in Figure 1 to the optical R -band with $\nu_{e,13} = 2$; this value is somewhat larger than the rough limit discussed in Figure 1 but may be consistent with the uncertainty in the model parameters. The model in the X-ray band is based on the measured¹⁴ optical to X-ray spectral slope and an extrapolation of the uniform density model presented in Figure 1. The sharp increase in the optical flux at $t \lesssim 1.5$ d is due to the deceleration of the slower second jet component. Finally, the dot-dashed line is the optical emission from SN 1998bw at the redshift of GRB 030329, $z = 0.1685$, used as a proxy for SN 2003dh.⁶ The solid line in the R -band is a combination of the SN and the two jet components, whereas in the radio and millimetre bands it is the uniform density model presented in Figure 1. In the X-ray band the model is dominated by the narrow jet component. While this two-component jet model provides a reasonable fit to the data, there are still some discrepancies which can be resolved by accurate photometry and a more careful subtraction of SN 2003dh. The latter will also allow a more precise determination of the putative second jet break in the optical band at $t_{j,\text{rad}}$.

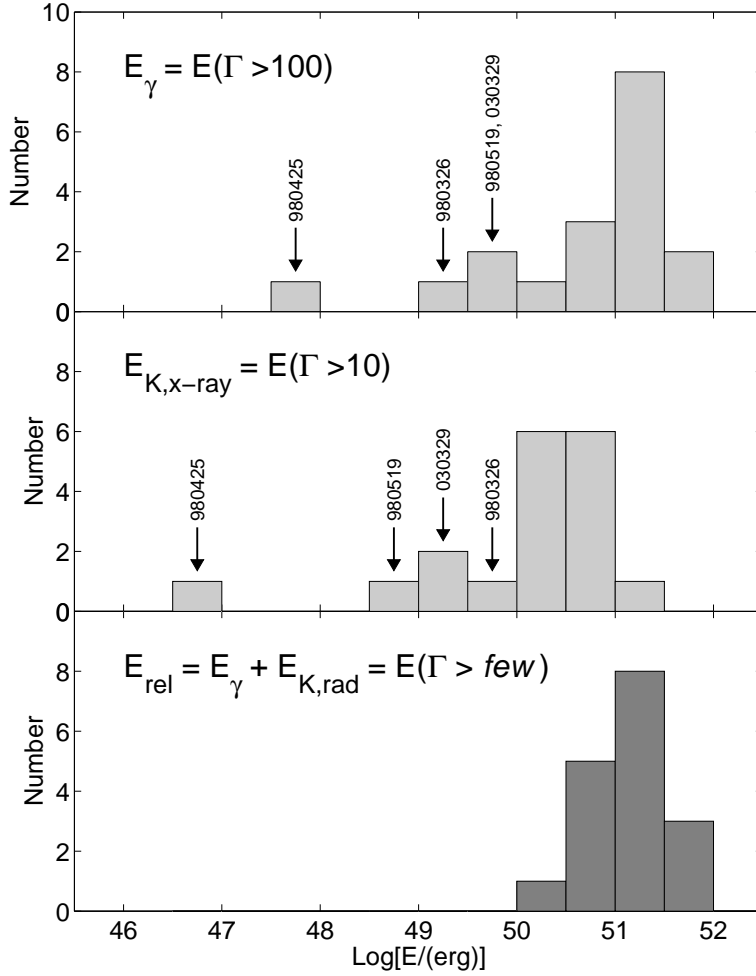


Figure 3. Histograms of various energies measured for GRBs. We plot the beaming-corrected γ -ray energy,³ E_γ , the kinetic energy inferred from X-rays at $t = 10$ hr,² $E_{K,X}$, and total relativistic energy, $E_{\text{rel}} = E_\gamma + E_K$, where E_K is the beaming-corrected kinetic energy inferred^{21,5} from the broad-band afterglow. The energy in X-rays, $E_{K,X} = L_X t / \epsilon_e (\alpha_X - 1)$, with $t = 10$ hr, $\epsilon_e = 0.1$, and $\alpha_X = 1.3$ is the median decay rate in the X-ray band. For GRB 980519 we find that the evolution of the radio emission requires a much wider jet, $\theta_j \sim 0.3$, than what is inferred from the optical, $\theta_j \sim 0.05$; here we assume $z = 1$. We therefore infer $E_K \sim 2 \times 10^{50}$ erg from the radio data compared to $E_\gamma \approx 4 \times 10^{49}$ erg. The γ -ray energy of GRB 980425 is an upper limit since the degree of collimation is not known. For the kinetic energy we use the value derived by Li & Chevalier²¹ based on the radio evolution of SN 1998bw. There is a significantly wider dispersion in E_γ and $E_{K,X}$ as compared to the total explosive yield. This indicates that engines in cosmic explosions produce approximately the same quantity of energy thus pointing to a common origin, but the quality of these engines, as indicated by ultra-relativistic output, varies widely.